Fusion Engineering and Design 98–99 (2015) 2103–2107

Contents lists available at ScienceDirect

Fusion Engineering and Design

journal homepage: www.elsevier.com/locate/fusengdes

Irradiation hardening in pure tungsten before and after recrystallization

Z.X. Zhang[a,*], D.S. Chen[a], W.T. Han[b], A. Kimura[b]

[a] Graduate School of Energy Science, Kyoto University, Gokasho, Uji, Kyoto, Japan
[b] Institute of Advanced Energy, Kyoto University, Gokasho, Uji, Kyoto, Japan

HIGHLIGHTS

- Grain morphology before and after recrystallization of tungsten was investigated by multiple methods.
- Hardening of tungsten irradiated under 6.4 MeV Fe^{3+} was investigated.
- Nano-indentation tests revealed that recrystallized tungsten with large grain sizes exhibits higher hardening effect than as-received.

ARTICLE INFO

Article history:
Received 26 September 2014
Received in revised form 20 June 2015
Accepted 26 June 2015
Available online 20 July 2015

Keywords:
Tungsten
Recrystallization
Ion-irradiation
Nano-indentation
Hardening effect

ABSTRACT

Ion-irradiation hardening of tungsten (W) before and after recrystallization was investigated in this paper. Three specimens were sampled from a rolled pure (99.95%) W plate. Two are from the as-received W and one was from the recrystallized W (annealed at 1400 °C for 1 h). Specimens were irradiated with 6.4 MeV Fe^{3+} at 300 °C, 700 °C and 1000 °C, respectively. The profile of displacement per atom (dpa) calculated by SRIM showed the average displacement damage is about 2 dpa at the depth of 600 nm. The hardness of irradiated area was measured by nano-indentation method with continuous stiffness measurement (CSM) and was calculated by Nix–Gao model for bulk-equivalent hardness. Irradiation hardening was defined as the difference between the hardness values of irradiated area and unirradiated area of a specimen. The result revealed that recrystallized specimens exhibited larger irradiation hardening than the as-received ones, and the amount of hardening was independent of irradiation temperature, while the hardening of as-received W increased with increasing irradiation temperature. There was no difference in the irradiation hardening between the specimens sampled from the different sides of the as-received W.

1. Introduction

Tungsten (W) is considered as armor material for diverter and blanket in fusion reactor as plasma facing materials [1–3]. Since the armor receives high heat loading and heavy neutron irradiation, the material may suffer irradiation hardening that is accompanied by loss of ductility. For the armor materials of divertor, the damage will accumulate to 15 dpa within 5 years in DEMO-like reactor with the operation temperature between 600 °C and 1300 °C [4]. Meanwhile, a transient flux up to 20 MW could cause recrystallization of W. Special designs and abundant experiments on W and its alloys have been required for diverter to endure such extreme conditions [5,6].

Tungsten and its alloys W-Re and W-Os are now widely researching. The irradiation effect of neutron has been investigated by several papers [7,8]. However, neutron source is too precious to obtain and long time consuming to achieve a certain damage level. Therefore, high energetic ion irradiation tests [9–14] were more popularly carried out to research the irradiation effect, especially the hardening effect, which presents for mechanical property, and also to research deuterium trapping behavior. With an ion-irradiation accelerator, DuET in Kyoto University, authors reported the hardening of W irradiated with Fe^{3+} at 500 °C up to a damage of 10 dpa [14]. Since it is expected that the irradiation temperature of plasma facing material reach to 1300 °C, recrystallization may occur in W and the irradiation effect at such a high temperatures is of interest. Since recrystallization results in grain growth, total grain boundary area is reduced and sink efficiency is affected. Furthermore, although the irradiation period was limited, there is a concern of precipitation of Fe_2W in the case of Fe^{3+} irradiation.

* Corresponding author.
E-mail address: zx-zhang@iae.kyoto-u.ac.jp (Z.X. Zhang).

http://dx.doi.org/10.1016/j.fusengdes.2015.06.192
0920-3796/

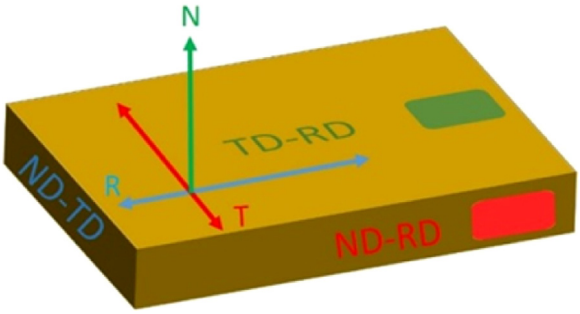

Fig. 1. Definition of different surfaces and directions. N stands for Normal, R stands for Rolling, T stands for Transverse direction. TD-RD (TR) means the surface parallel to T and R direction.

In this paper, we focused on the irradiation temperature dependence of the hardening of pure W before and after recrystallization.

2. Experiment

The material used was the as-received pure W (99.95%) supplied by Nilaco Corporation in hot rolled condition. EBSD analysis and SEM observation was performed on FE-SEM (ZEISS Ultra55) equipped with EBSP. The different surfaces were defined by Fig. 1, RT stands for the rolling surface while NR and NT stand for the side surface respectively. Isochronal annealing for 1 h at different temperatures was performed followed by Vickers hardness tested using ASAHI HM-103-HH at 0.1 kgf kept for 10 s. As for irradiation hardening measurement, nano-indentation was carried out by G200 Agilent Tech. with a berkovich tip and measured by continuous stiffness measurement (CSM) method with 1 nm oscillation and maximum 2 μm indent depth.

Three types of specimens were prepared for irradiation. TR and NR indicates that the irradiation beam is normal to the surface of TD-RD (TR) and ND-RD (NR) surfaces, respectively. As for the investigation of the effect of recrystallization on irradiation hardening, a specimen was annealed at 1400 °C for 1 h (named as RE) and the beam direction is normal to the TR surface.

All the specimens were mechanically polished with SiC paper from #500 to #2500, followed by buffer polishing with diamond pastes with diameters up to 0.025 micron. The samples were finally electrically polished in a 0.5 N NaOH solution for 2 min at room temperature. The voltage was 13 V.

Irradiation experiments were carried out in the year 2014. The specimens were irradiated by DuET in Kyoto University with 6.4 MeV Fe^{3+} ions. The flux was controlled at about 1.25×10^{16} ion/m^2/s, and the total irradiation times were about 67 min. The irradiation temperatures were 300 °C, 700 °C, 1000 °C, which were monitored by infrared thermal vision. The damage was simulated by SRIM code 2013 [15] using "Quick calculation of Damage" mode. The threshold was set at 90 eV [16,17], and lattice binding energy is null. There are two methods to calculate the profile of displacement per atom (dpa): (1) Traditional QD method, which calculated by the vacancies. (2) Energy damage (ED) method, which calculated the Frenkel pair by the energy loss to ions and recoils using the NRT model equation [18], the T_{dam} is the damage energy, equals the sum of beam energy and target atom energy lost to phonons.

$$\nu_{NRT} = \frac{0.8T_{dam}}{2E_d} \quad (1)$$

Even though the difference between these two methods is very small, the ED method was recommended to avoid the vacancy model of SRIM, which is considered to contain a big error [19]. The result reveals that the peak damage 4 dpa appears at 1200 nm and the average 2 dpa is estimated at the depth of 600 nm. The projected range is about 2 μm (Fig. 2).

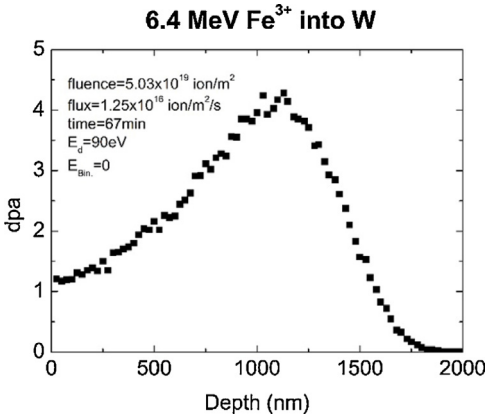

Fig. 2. The depth profile of dpa calculated by SRIM by the energy damage method.

3. Results and discussion

3.1. Recrystallization temperature determination

Fig. 3(a) shows the Vickers hardness changes during isochronal annealing for 1 h. The hardness remains stable up to 1200 °C but sharply decreases at 1300 °C and 1350 °C. When it comes to 1400 °C, the hardness decreases a little. Fig. 3b, c, d also show the EBSD results on grain morphology including misorientation of attached grains. In as-received condition, grain size is rather small with large proportion of small misorientation below 15°. At 1300 °C, some of the grains extremely grew, and the misorientation was mainly above 15°, but there are still small grains and grain boundaries with small misorientation. At 1400 °C, only large grains and very few grain boundaries with small misorientation were found. Therefore, the W after annealing at 1300 °C for 1 h is considered to be partially recrystallized, while the W annealed to 1400 °C is fully recrystallized.

3.2. Grain morphology and texture

The differences in microstructure for these three type of specimens are mainly grain morphologies and textures. The SEM images shown in Fig. 4 indicates that the grains are homogeneous on the TR surface of as-received specimen. On the NR surface, the grains were elongated to the rolling direction. The recrystallized samples showed large equiaxial grains. The grain sizes are compared in Table 1. For as-received W which was simply presented by the orientation distribution function (ODF) with $\varphi_2 = 45°$. The figure shows a high area ratio of (1 1 0)[1 1 0] texture besides some (1 1 2)[1 1 0] and (1 1 0)[1 1 2], which means that the main texture is (1 0 0)[1 1 0] on the rolling surface TR, and there are a few textures of (1 1 0)[1 1 0] and (1 1 0)[1 1 2].

3.3. Irradiation hardening

Since damage depth is about 2 μm, which is not deep enough to test with an ordinary Vickers hardness tester, nano-indentation with CSM mode [20] was carried out to measure the irradiation hardening. Fig. 5 shows that all of the irradiated specimens indicate irradiation hardening even at 1000 °C. The hardness after irradiation at 700 °C is largest and the hardness also decreased rapidly with increasing indentation depth. The hardness profiles of the

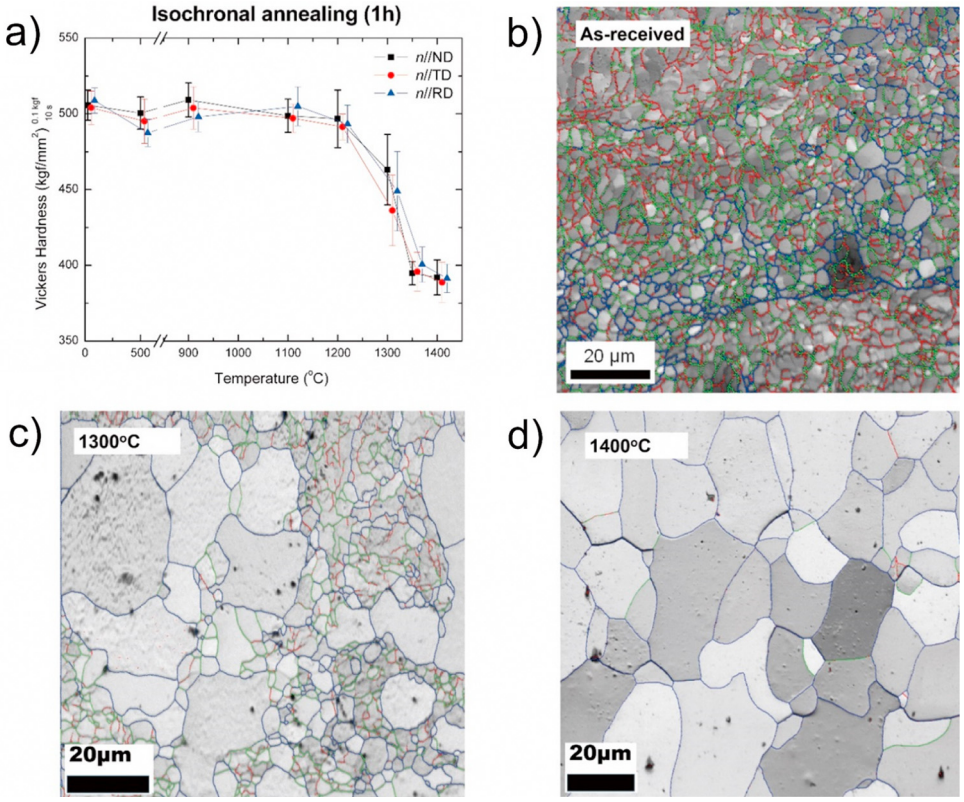

Fig. 3. (a) Vickers hardness changes by isochronal annealing for 1 h. The grain morphology of (b) as-received, (c) annealed at 1300 °C and (d) 1400 °C. Colors of grain boundaries stand for misorientation: (1) blue >15° (2) green 5–15° (3) red <5°. (For interpretation of the references to color in this figure legend, the reader is referred to the web version of this article.)

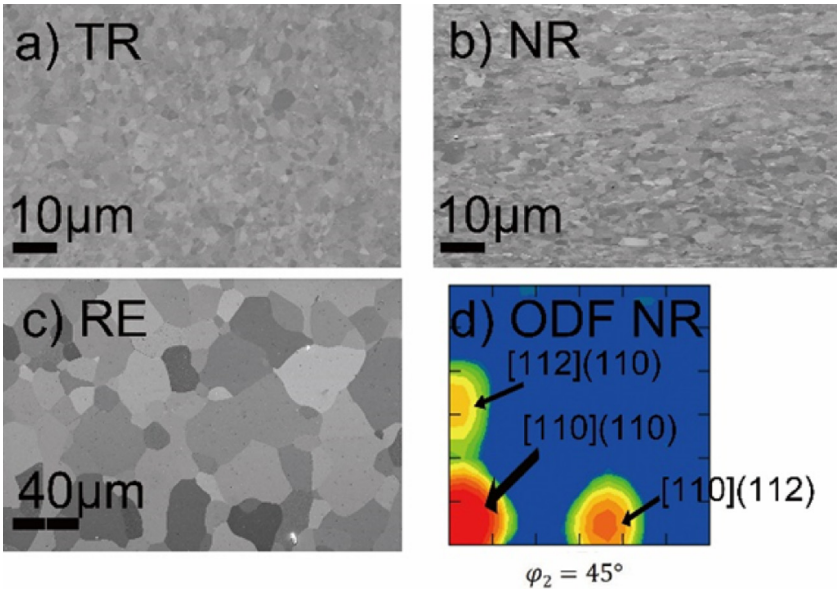

Fig. 4. SEM image of grain sizes: (a) TR, (b) NR, (c) RE and ODF at $\varphi_2 = 45°$ of NR surface of as-received tungsten.

Table 1
Summary of the grain sizes and nano-hardness.

	Grain size (μm)			Nano-hardness (GPa)									
	Length	Width	Rate	Unirr	300 °C			700 °C			1000 °C		
					Irr.	Unirr	ΔH	Irr.	Unirr	ΔH	Irr.	Unirr	ΔH
TR	1.65	1.73	0.96	6.13	7.13	6.05	1.09	7.26	5.85	1.41	7.69	6.07	1.62
NR	1.88	0.98	1.92	6.17	7.51	6.43	1.08	7.59	6.14	1.45	7.55	5.95	1.60
RE	30	23	1.29	5.16	7.18	5.04	2.14	7.28	5.16	2.12	7.19	5.07	2.12

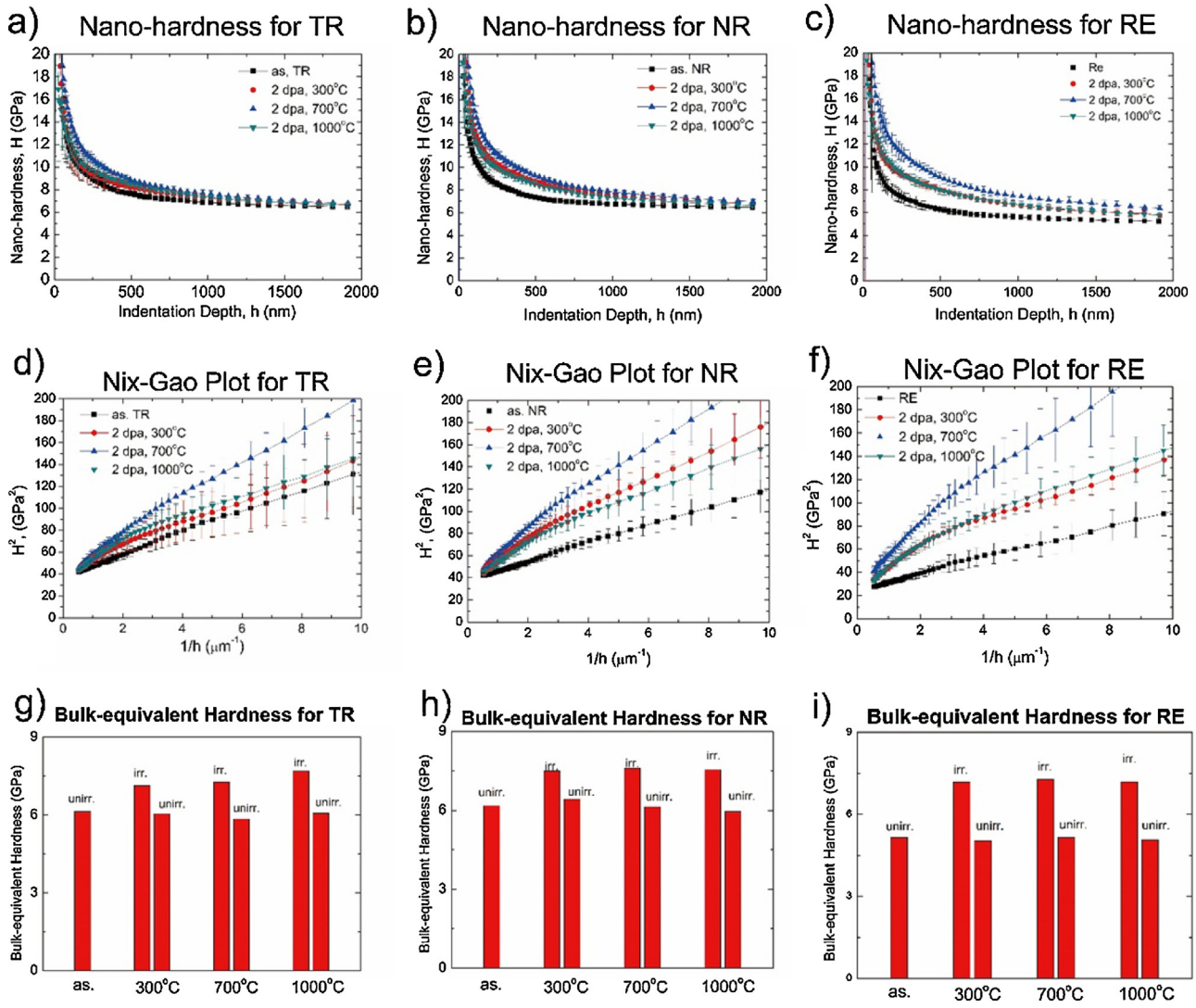

Fig. 5. Nano-indentation hardness results of irradiated samples tested by CSM mode: as-received (a) TR, (b) NR surface and (c) recrystallized condition. Each graph includes hardness in the damage area up to nominal 2 dpa at 300 °C, 700 °C, 1000 °C and before irradiation. Nix–Gao plot for (d) TR (e) NR (f) RE were showed before and after irradiation. Bulk-equivalent hardness evaluated by Nix–Gao model of (g) TR, (h) NR, (i) RE. Irr. stands for the bulk-equivalent hardness tested on irradiated area and Unirr stands for the bulk-equivalent hardness tested on un-irradiated area at different temperatures.

specimens irradiated at 300 °C and 1000 °C were similar. All of the irradiated samples showed hardening effect.

Bulk-equivalent hardness was evaluated by Nix–Gao model [21] (Eq. (2)) considering indentation size effect [22] and softer substrate effect [23]. The irradiation effect was calculated by bulk-equivalent of irradiation area minus the un-irradiated area. The results are listed in Table 1.

$$H = H_0\sqrt{1 + \frac{h_c}{h}} \tag{2}$$

The recrystallized specimens exhibited a larger irradiation hardening than as-received ones, and the hardening did not show significant changes in the present temperature range. The larger irradiation hardening is considered to be due to reduction of grain boundary area. Since grain boundaries play a role as sink sites for damage structures, a large amount of interstitial atoms and vacancies will be survived during irradiation. Most of these interstitial atoms and vacancies will recombine or absorbed by lattice defects, for example, grain boundaries. But the remained defects will form into dislocation/loops, voids, precipitates or other irradiation induced structures. For example, the loops could act as obstacles that block the dislocation motion, and therefore resulting in strengthening [24]. TEM observation revealed that a large amount of voids were found in all the specimens irradiated at 1000 °C, but no obvious void was found in the specimens irradiated at 300 °C and 700 °C, while a number of dislocation loops were observed in all the specimens irrespective of irradiation temperature. Therefore, it is considered that not the voids but dislocation loops are the main contributor of the hardening. The contribution of these structures to the hardening effect could be estimated by Orowan type equations, and will be reported in elsewhere. It can be noticed that the irradiation hardening of as-received ones increased as irradiation temperature increased, which can be explained in terms of growth of the dislocation loops with increasing the temperature. The irradiation hardening effect showed no significant difference on rolling surface (TR) and side surface (NR) in the experiment temperature range.

4. Conclusion

The recrystallization temperature of the rolled as-received W was evaluated to be 1400 °C as fully recrystallization temperature.

The grain morphology and textures were researched. Main texture of (1 0 0)[1 1 0] was determined of the rolling surface (TR). The grains were elongated on the side surface (NR) but equiaxial on the rolling top surface (TR).

Pure W in as-received and recrystallized condition were irradiated by 6.4 MeV Fe^{3+} at 300 °C, 700 °C, 1000 °C up to 2 dpa. Irradiation hardening effect was observed at all the temperatures. The recrystallized W showed a larger irradiation hardening effect than as-received ones, which is considered to be due to the reduction of grain boundary area that plays a role as a sink site. As temperature increased, the irradiation hardening effect of as-received ones increased, while the hardening of recrystallized W is independent of irradiation temperature. There was no difference in the irradiation hardening effect between the specimens sampled from the different sides of the as-received W.

Acknowledgments

The first author gratefully acknowledges the China Scholarship Council who offers the financial support. Dr. Ha Yoosung of Institute of Advanced Energy, Kyoto University is gratefully acknowledged for the technical support of hot-press furnace and nano-indenation operation. Additionally, Dr. Chen Siwei of Graduate School of Engineering, Hokkaido University is thanked for her professional advisement.

References

[1] P. Norajitra, et al., Development of a helium-cooled divertor: material choice and technological studies, J. Nucl. Mater. 367–370 (2007) 1416–1421.
[2] P. Norajitra, et al., He-cooled divertor for DEMO: experimental verification of the conceptual modular design, Fusion Eng. Des. 81 (2006) 341–346.
[3] G. Janeschitz, et al., Development of fusion technology for DEMO in Forschungszentrum Karlsruhe, Fusion Eng. Des. 81 (2006) 2661–2671.
[4] H. Bolt, et al., Plasma facing and high heat flux materials – needs for ITER and beyond, J. Nucl. Mater. 307–311 (2002) 43–52.
[5] M. Rieth, et al., Recent progress in research on tungsten materials for nuclear fusion applications in Europe, J. Nucl. Mater. 432 (2013) 482–500.
[6] M. Rieth, et al., Review on the EFDA programme on tungsten materials technology and science, J. Nucl. Mater. 417 (2011) 463–467.
[7] A. Hasegawa, et al., Neutron irradiation effects on tungsten materials, Fusion Eng. Des. 89 (2014) 1568–1572.
[8] A. Hasegawa, et al., Neutron irradiation behavior of tungsten, Mater. Trans. 54 (4) (2013) 466–471.
[9] M.H. Cui, et al., Temperature dependent defects evolution and hardening of tungsten induced by 200 keV He-ions, Nucl. Instrum. Methods Phys. Res. B 307 (2013) 507–511.
[10] X. Yi, et al., In situ study of self-ion irradiation damage in W and W-5Re at 500 °C, Philos. Mag. 93 (14) (2013) 1715–1738.
[11] H. Wang, et al., Effect of high fluence Au ion irradiation on nanocrystalline tungsten film, J. Nucl. Mater. 442 (2013) 189–194.
[12] V.Kh. Alimov, et al., Hydrogen isotope exchange in tungsten irradiated sequentially with low-energy deuterium and protium ions, Phys. Scr. T145 (2011) 014037, 5 pp.
[13] D.E.J. Armstrong, et al., Hardening of self ion implanted tungsten and tungsten 5-wt% rhenium, J. Nucl. Mater. 432 (2013) 428–436.
[14] Y. Himei, et al., Ion-irradiation hardening of brazed joints of tungsten and oxide dispersion strengthened (ODS), Mater. Trans. 54 (4) (2013) 446–450.
[15] http://www.srim.org/
[16] ASTM E521-96: 2009 Standard Practice for Neutron Radiation Damage Simulation by Charged-Particle Irradiation.
[17] Q. Xu, T. Yoshiie, H.C. Huang, Molecular dynamics simulation of vacancy diffusion in tungsten induced by irradiation, Nucl. Instrum. Methods Phys. Res. B 206 (2003) 123–126.
[18] M.J. Norgett, M.T. Robinson, I.M. Torrens, A proposed method of calculating displacement dose rates, Nucl. Eng. Des. 33 (1) (1975) 50–54.
[19] R.E. Stoller, et al., On the use of SRIM for computing radiation damage exposure, Nucl. Instrum. Methods Phys. Res. B 310 (2013) 75–80.
[20] W.C. Oliver, G.M. Pharr, An improved technique for determining hardness and elastic modulus, J. Mater. Res. 7 (6) (1992) 1564–1583.
[21] W.D. Nix, H.J. Gao, Indentation size effects in crystalline materials: a law for strain gradient plasticity, J. Mech. Phys. Solids 46 (3) (1998) 411–425.
[22] G.M. Pharr, E.G. Herbert, Y. Gao, The indentation size effect: a critical examination of experimental observations and mechanistic interpretations, Annu. Rev. Mater. Res. 40 (2010) 271–292.
[23] R. Kasada, et al., A new approach to evaluate irradiation hardening of ion-irradiated ferritic alloys by nano-indentation techniques, Fusion Eng. Des. 86 (2011) 2658–2661.
[24] R.O. Scattergood, D.J. Bacon, Acta Metall. 30 (1982) 1665–1677.